

AERODYNAMIC SEPARATION OF FRAGMENTED BODIES IN HIGH-SPEED FLOW

Advanced Modeling & Simulation (AMS) Seminar Series
NASA Ames Research Center, September 23rd, 2021

Tom Whalen

NASA NSTRF Fellow / University of Maryland



A. JAMES CLARK
SCHOOL OF ENGINEERING

DEPARTMENT of
AEROSPACE ENGINEERING



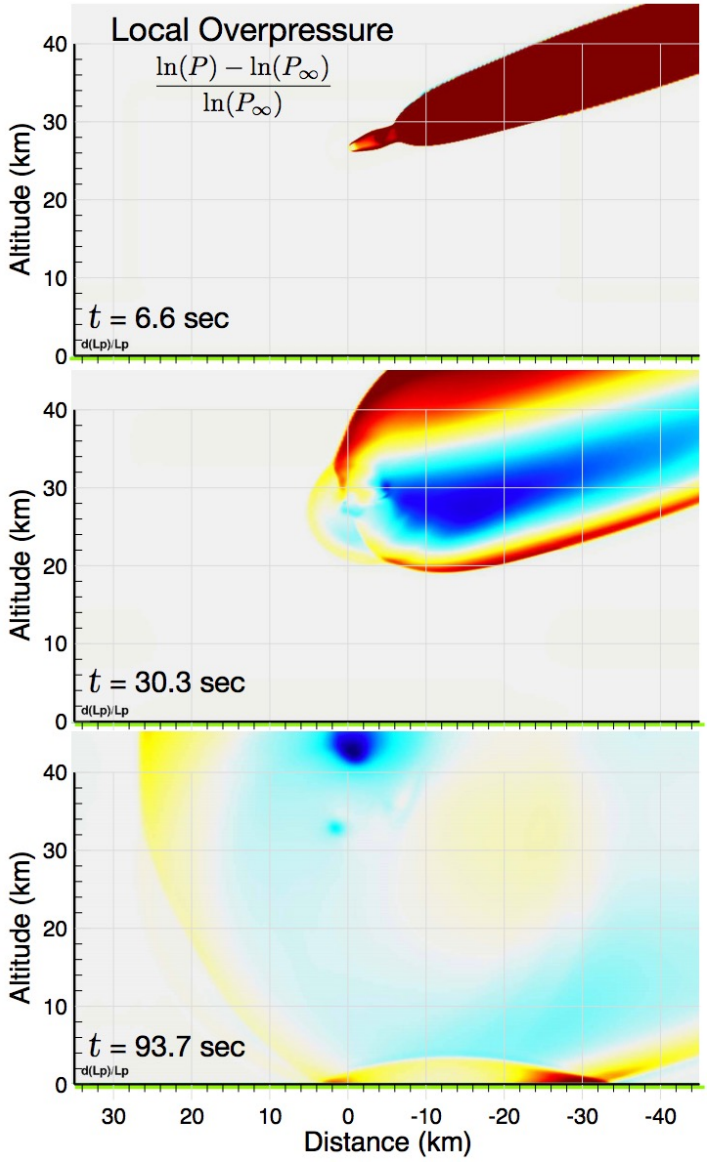
Outline

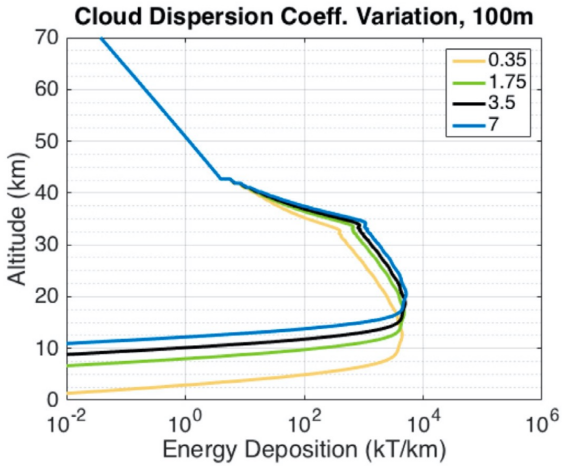
- Motivation/Approach
- Methodology
- Equal-Sphere Clusters
- Unequal-Sphere Clusters
- Dusty Debris
- Conclusions

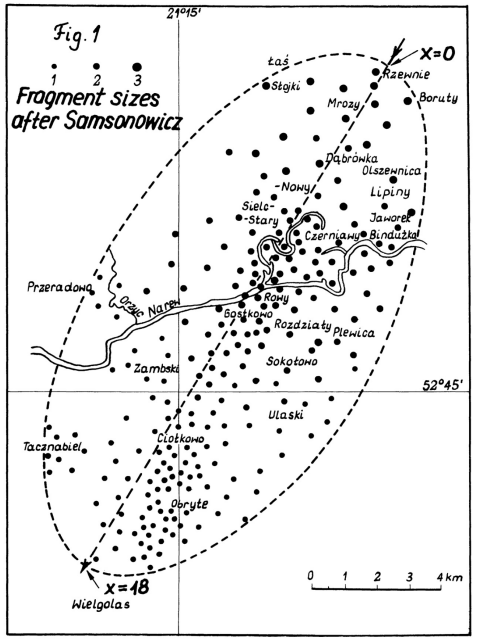


Motivation

- Meteors and asteroids entering Earth's atmosphere have potential for catastrophic ground damage
- Energy deposition, strewn field morphology highly correlated to flow physics of fragmenting body
- **Need accurate description of separation aerodynamics for adequate risk assessment**





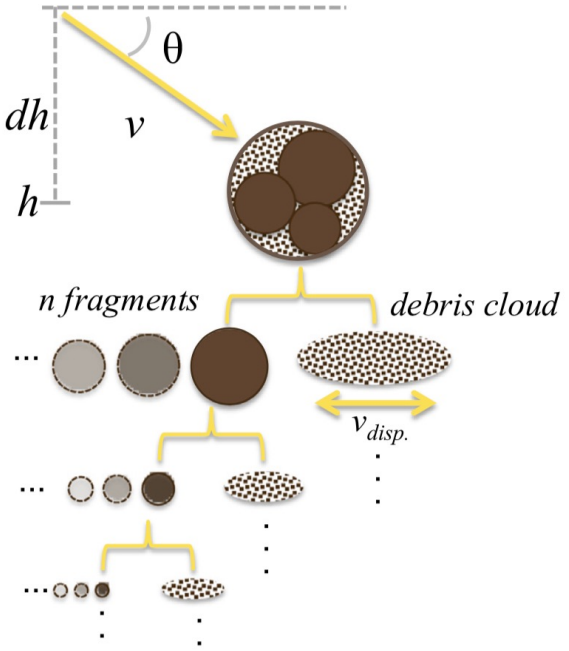


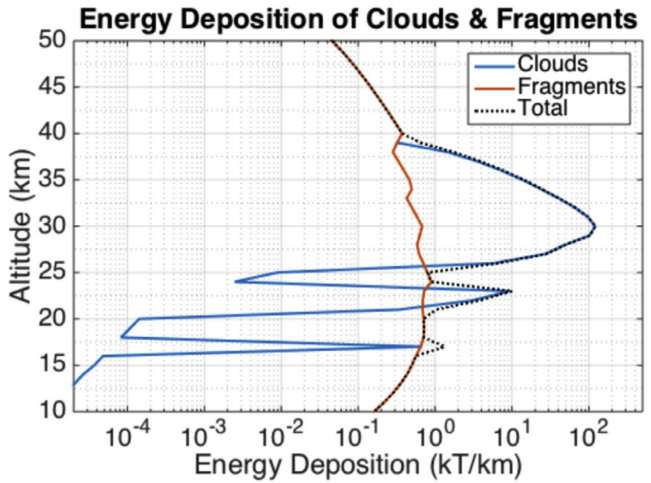
CW from top-right: Wheeler et al., 2017; Lang and Kowalski, 1974; Aftosmis et al., 2016

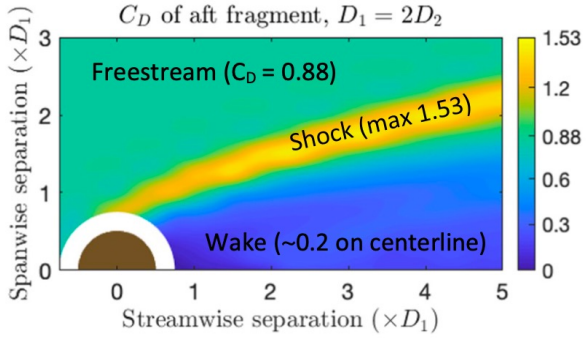
Modeling

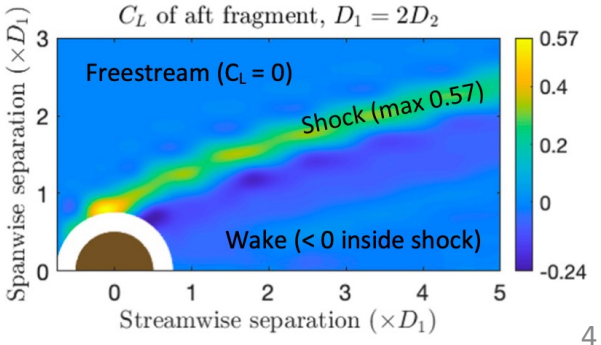
- Energy deposition models:
  - Liquid/pancake model, discrete fragment, hybrid
  - Calibration from specific entry events
- Aerodynamic models:
  - Analytical, semi-analytical, and database
  - All specifically designed for sphere pairs
  - Validity for scenarios with additional bodies not guaranteed
  - Necessary for ground footprint prediction

Left: Wheeler et al., 2017;
right: Register et al., 2017;
bottom: Register et al., 2020





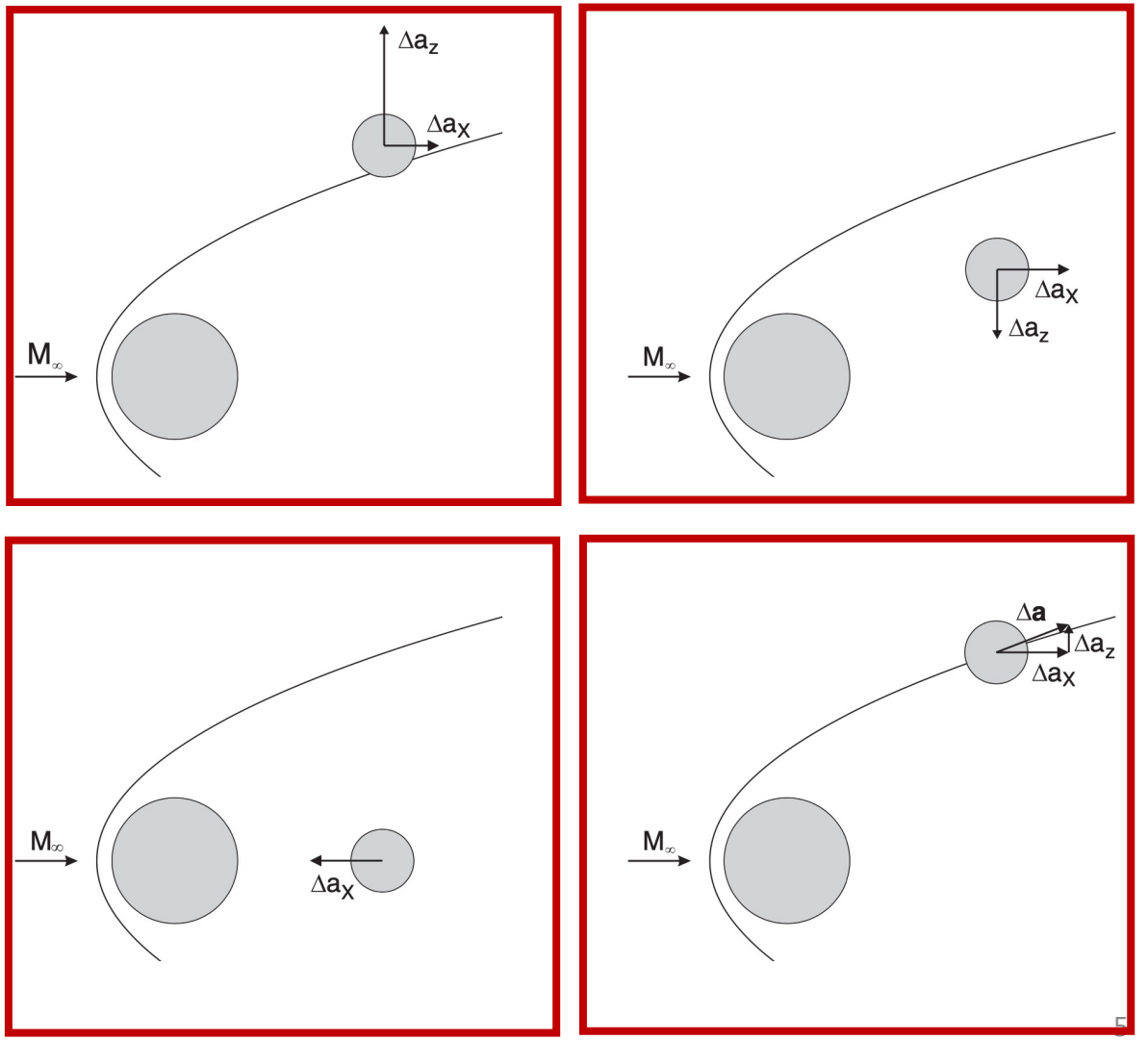




Marwege, 2018

Sphere Pair Dynamics

- Four general behaviors for sphere pairs:
  - Expulsion
    - Also from lateral initially touching positions
  - Entrainment
    - Far wake flight
    - OR transition into drafting
  - Drafting
    - Leads to collision for equal spheres
  - Shock surfing
    - Highly enhances separation velocity



Model Problem

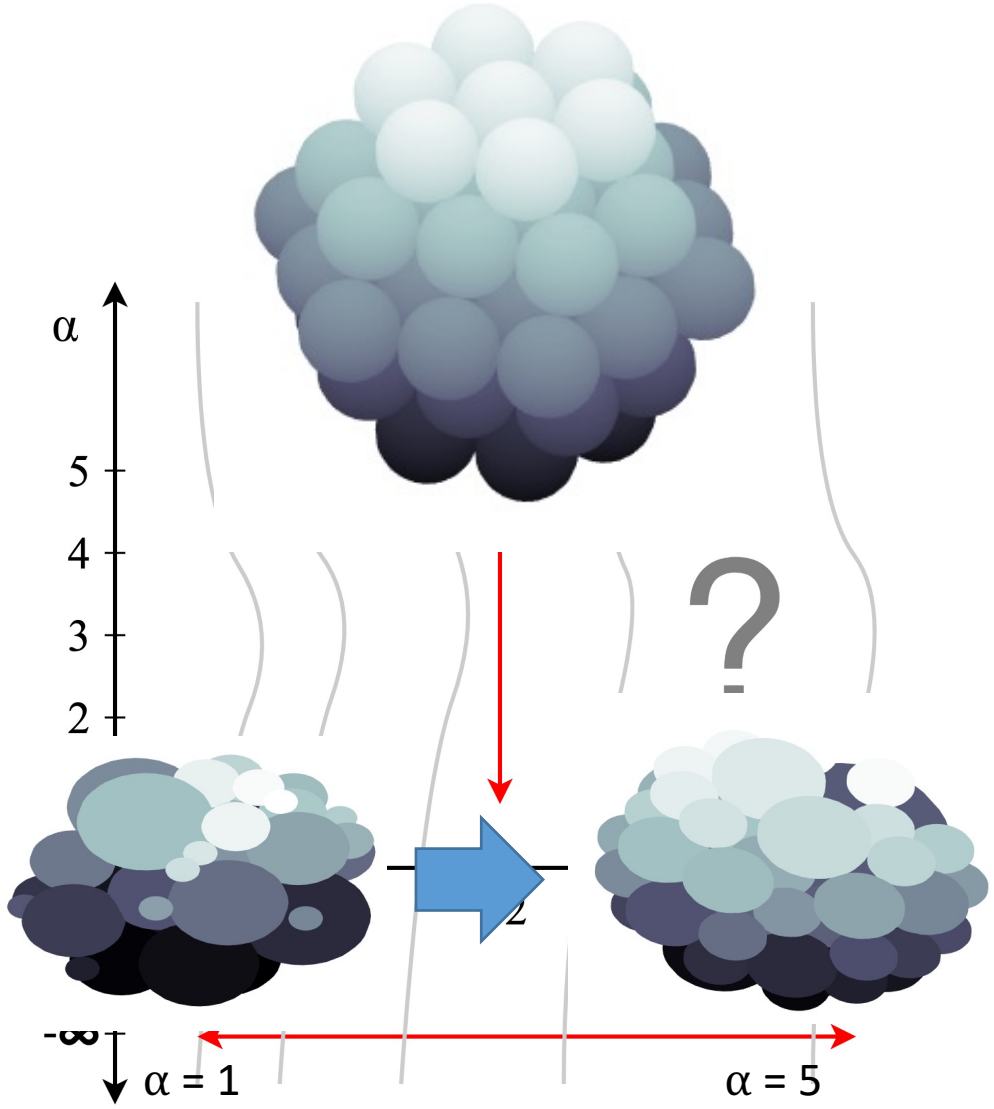
- Examine simplified multi-body problem with following constraints
  1. **All fragments are perfect spheres**
  2. **Initially close-packed into surrounding sphere**
  3. **Fragmentation is instantaneous**
  4. **No dusty debris released at fragmentation**
  5. No strain energy released (i.e., bodies stationary w.r.t. each other)
  6. No further fragmentation occurs before bodies are independent
  7. Overall cluster is rotationally stationary
  8. **All dynamics occur under perfect-gas, hypersonic flow**
  9. Constant inflow conditions

Parameters of Study

- Within scope of model problem, two parameters dictate separation behavior of fragmented cluster

1. Population (equal-sphere clusters)
   - N varies between 2 and 115
2. Fragment-size distribution (unequal-sphere clusters)
   - Agglomeration selected according to power-law distribution: $p(r) = A\, r^{-\alpha}$, $r_{max}/r_{min} = 4$
   - α values between 1 and 5 chosen, fixed N

- Defines plane of separation behaviors



Strategy and Objectives

- Complementary approach with both experiments and simulations
- Experiments
  - Free-flight tests in short-duration facility -> approximation of idealized release
  - Random cluster arrangements
  - Assessment of populous and unequal sphere clusters
  - Focus on statistics of terminal trajectories for many configurations
- Simulations
  - Idealized release of clustered bodies into freestream from well-defined initial positions
- Questions to address:
  - What happens when a meteoroid breaks into more than two fragments?
  - Are new physical mechanisms introduced?
  - Can we develop statistical separation models of lateral fragment spread?
  - Relaxing our constraints, how do dusty debris clouds behave in high-speed flows?

Important Definitions

- Lateral separation velocity from system center-of-mass a critical quantity:

$$v_s = \sqrt{\frac{\rho_\infty}{\rho_{\text{sph}}}} u_\infty, \qquad V_T' = V_T / v_s, \qquad \overline{V_T'} = \overline{V_T} / v_s$$

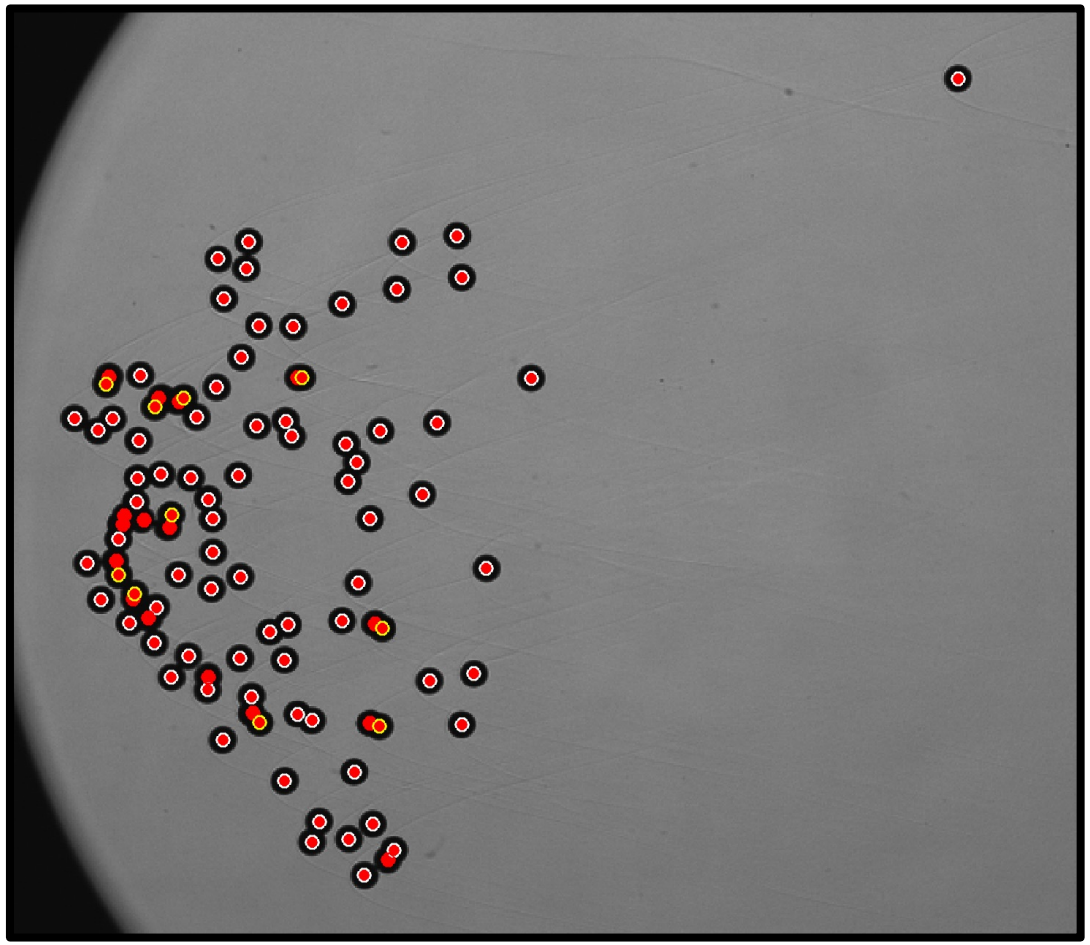
- Nondimensional time:

$$\tau_s = \sqrt{\frac{\rho_{\text{sph}}}{\rho_\infty} \frac{r_c}{u_\infty}} \qquad t' = t / \tau_s$$

Source	Scenario	V_T' Range
Passey and Melosh (1980)	2 unequal spheres	0.14 – 1.23
Hills and Goda (1993)	Debris cloud	1.8
Artemeva et al. (1996)	2 equal hemicylinders	0.31
Artemeva et al. (2001)	13 equal cubes	0.71
Laurence et al. (2012)	2 unequal spheres	0.22 – 1.0
Park et al. (2020)	2 – 6 equal spheres	$(0.032\ \text{N})^{0.5}$

Outline

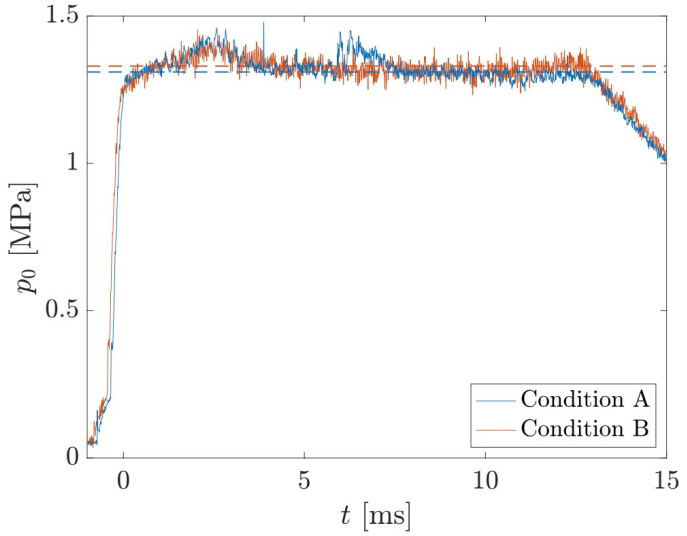
- Motivation/Approach
- Methodology
- Equal-Sphere Clusters
- Unequal-Sphere Clusters
- Dusty Debris
- Conclusions

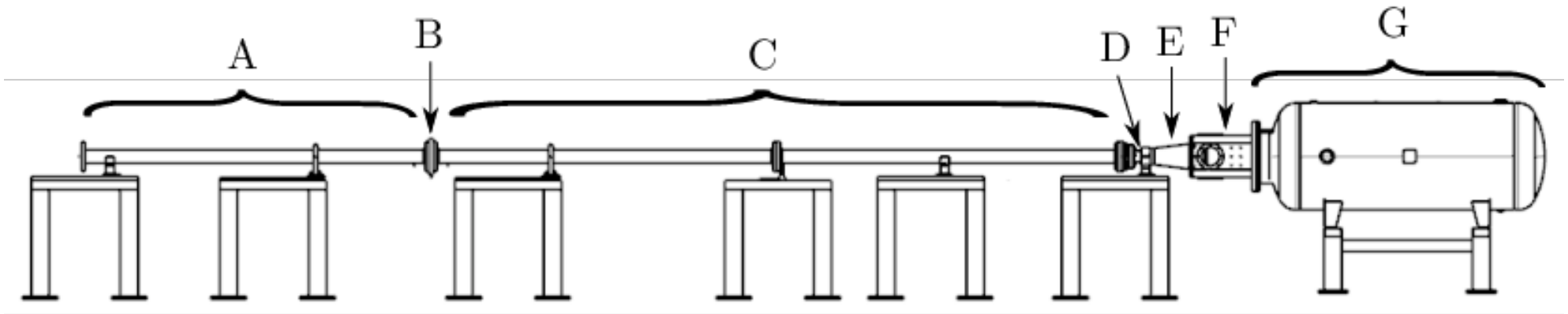


Experimental Facility

	Condition A	Condition B
M_∞	6.0	6.05
P_∞ [Pa]	790	847
T_∞ [K]	110	112
ρ_∞ [kg/m^3]	0.0249	0.0263
u_∞ [m/s]	1264	1275

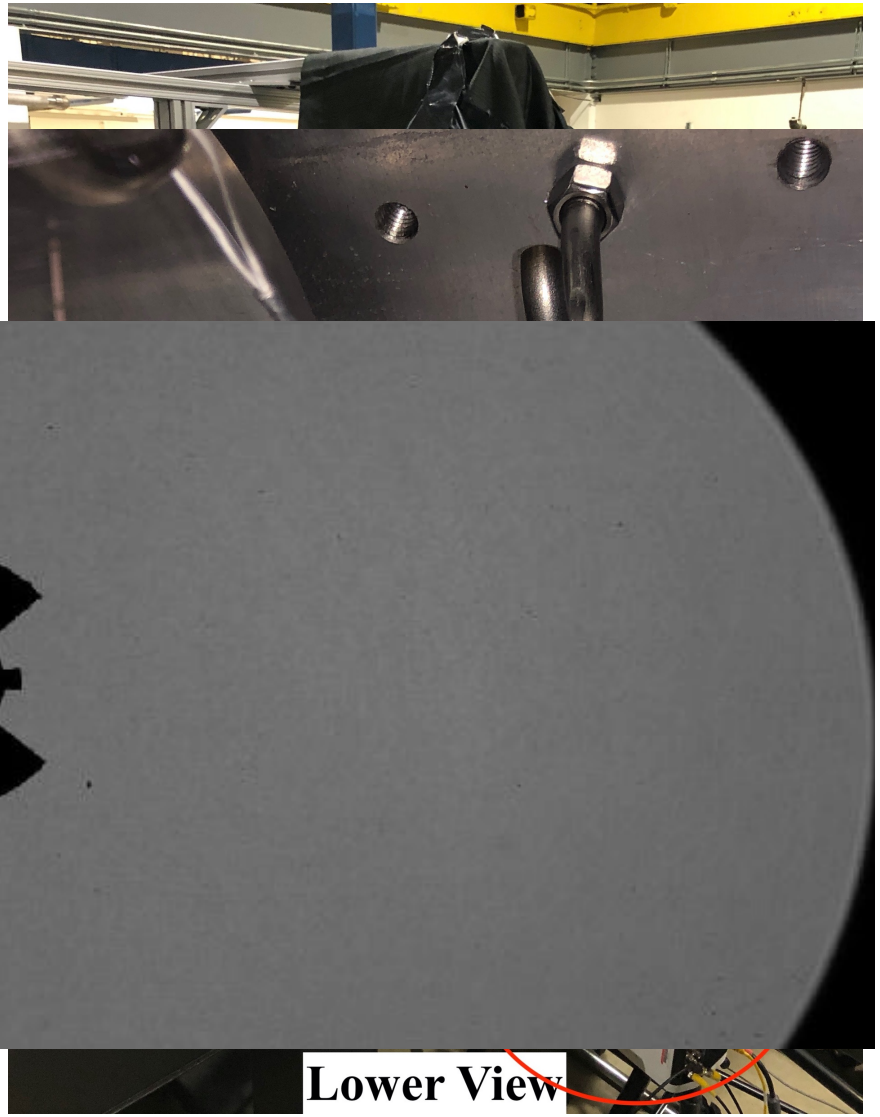
- UMD HyperTERP: shock tunnel with dried air/nitrogen
- Mach 6 contoured nozzle
- Fill conditions tailored for ~13 ms test duration
- Two sets of freestream conditions utilized
  - Pressure unsteadiness limited to 3.5% (1.5% run-to-run)
  - Short pressure rise time





Butler and Laurence, 2019

Visualization and Release



- Finite difference of position to extract velocity

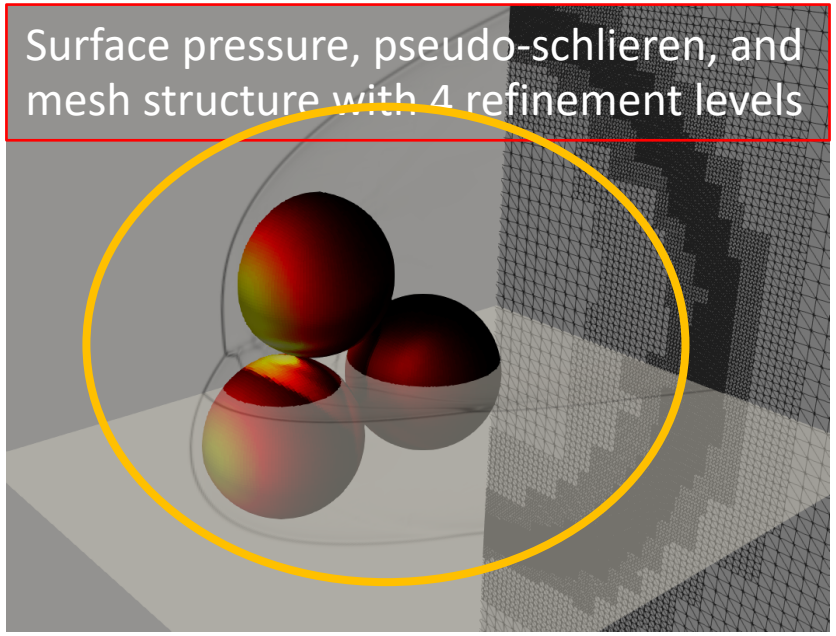
Cluster Configurations

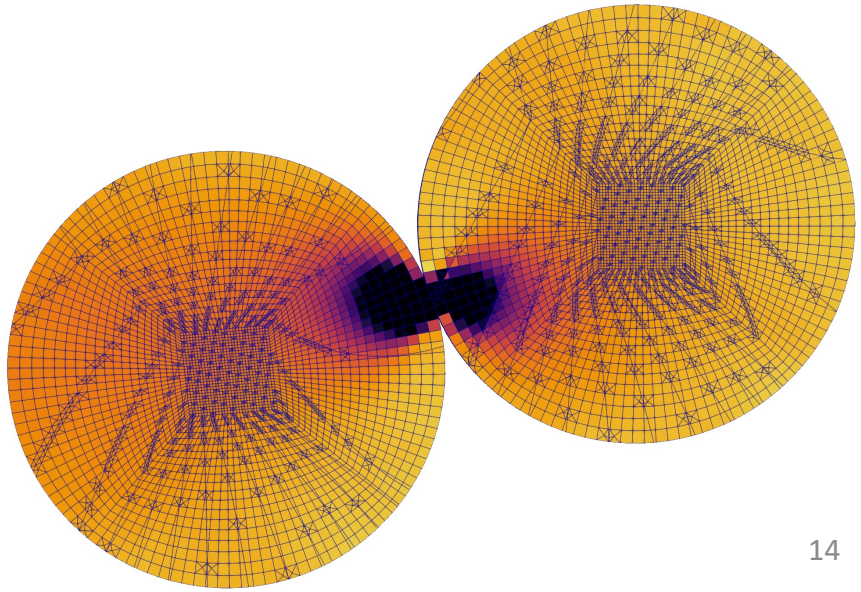
- In total, 67 useful wind tunnel tests conducted
  - Populations from successive increases of 90%, intermediate cases for completeness

N	d_{sph} [mm]	d_c [mm]	Material	Flow Config.	# Upstream Runs	# Downstream Runs	Camera Config.
4	5.0 / 6.35	11 / 13.9	PTFE / Delrin	A / B	0	5	C3 / C1
8	5.0 / 5.56	13 / 15.2	PTFE / Delrin	A	3	2	C3 / C2
11	4.76	13.6	PTFE	B	0	2	C1
14	4.76	15.2	Delrin	A	4	0	C2
15	5.0	15.3	PTFE	A	0	4	C3
27	4.0	15.2	Delrin	A	4	1	C2
36	3.18	13.9	Delrin	B	0	1	C1
52	3.18	15.2	Delrin	A	4	1	C2
52	$\alpha = 1$	17.5	Delrin	A	4	1	C2
52	$\alpha = 2$	14.4	Delrin	A	4	1	C2
52	$\alpha = 3$	17.9	Delrin	A	4	1	C2
52	$\alpha = 4$	15.2	Delrin	A	4	1	C2
52	$\alpha = 5$	13.6	Delrin	A	4	1	C2
99	2.38	13.9	Delrin	A	1	0	C2
115	2.38	13.9	Delrin	A	4	1	C2
$\gg 115$	~ 0.020	13.9	Cornstarch Powder	A	2	3	C2

Fluid-Structural Solver

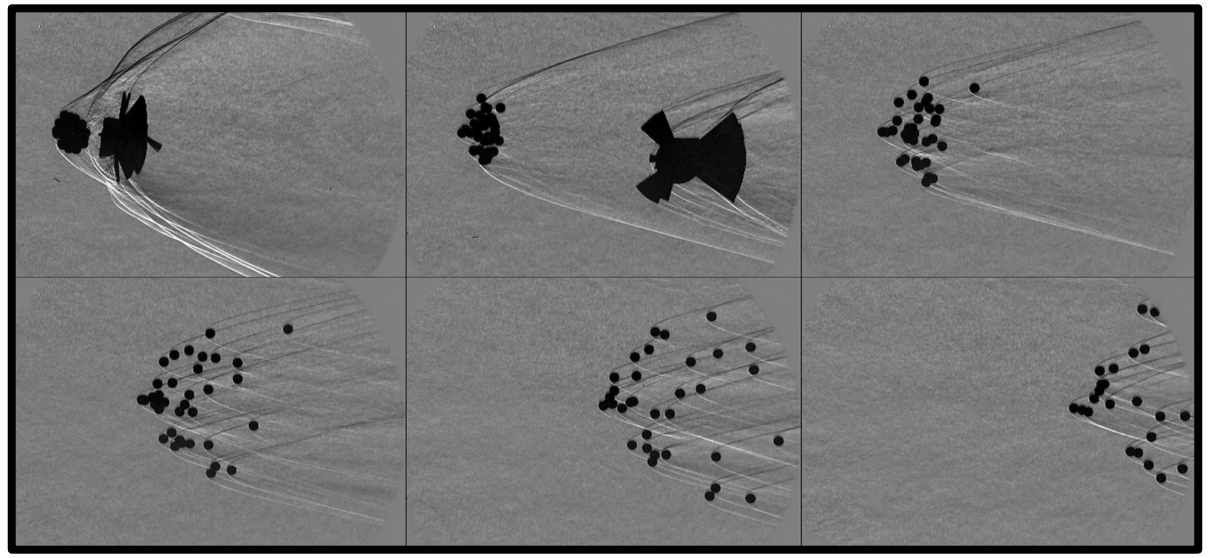
- AMROC (Adaptive Mesh Refinement in Object-Oriented C++):
  - Solves Euler equations with explicit, FV approach
  - MUSCL-Hancock with Minmod limiter and Van Leer flux vector splitting
  - Block-structured AMR on Cartesian mesh
- DYNA3D:
  - Nonlinear FEA solver with wide range of available material models (use elastic only)
  - Robust contact detection algorithm
- Methodology validated w/ experiments, verified w/ grid refinement
- 2-, 4-, 13-, and 57-equal-sphere clusters





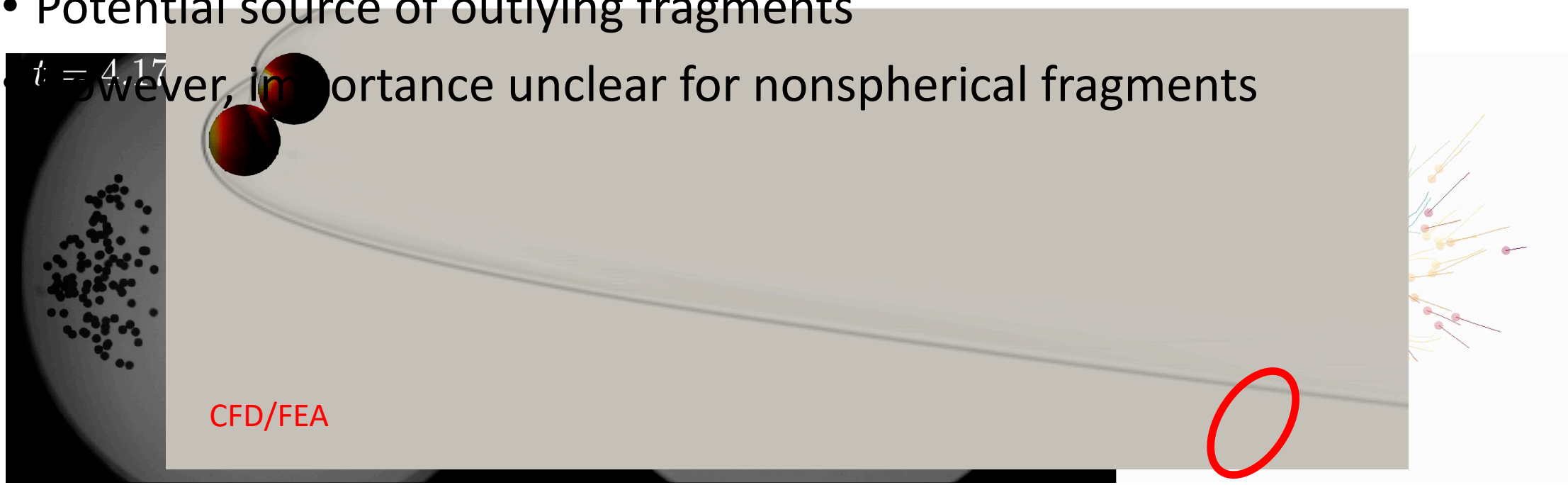
Outline

- Motivation/Approach
- Methodology
- Equal-Sphere Clusters
- Unequal-Sphere Clusters
- Dusty Debris
- Conclusions



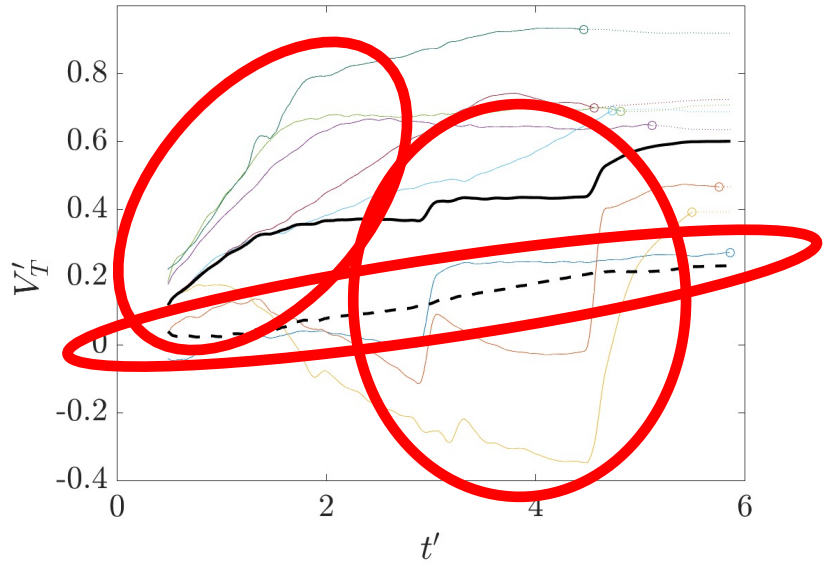
Stable Sphere Pairs

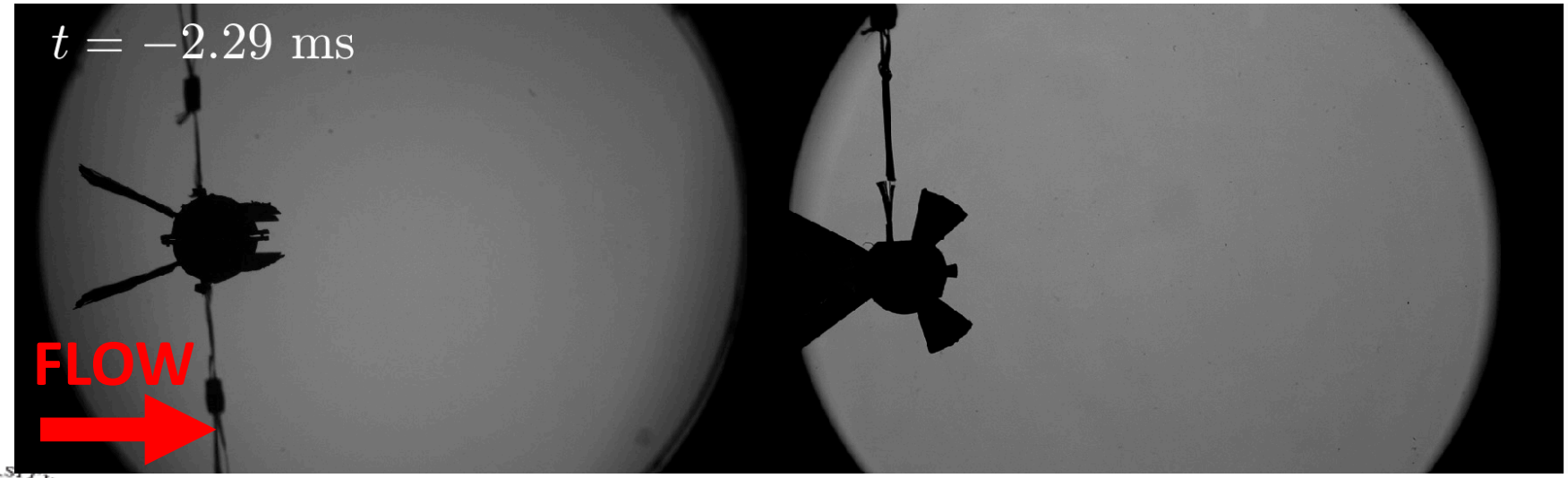
- For certain alignment angles, quasi-stable arrangement with restorative moment and effective lift
- Potential source of outlying fragments
- However, importance unclear for nonspherical fragments



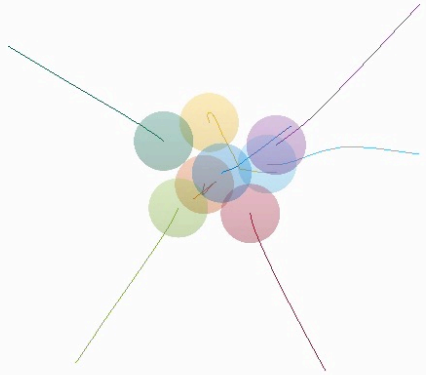
Primary vs. Secondary Separation

- 8 equal spheres → distinct separation regimes
  - Primary phase: Initial repulsion provides nearly linear velocity increase
  - Secondary phase: Collisions help disrupt cluster ‘core’, increase lateral range of fragments by 40%
  - System center-of-mass shifted off-axis
- Separation process divided into two stages, must expand ground footprint for CoM deflection
- Importance of secondary interactions reduced with more bodies



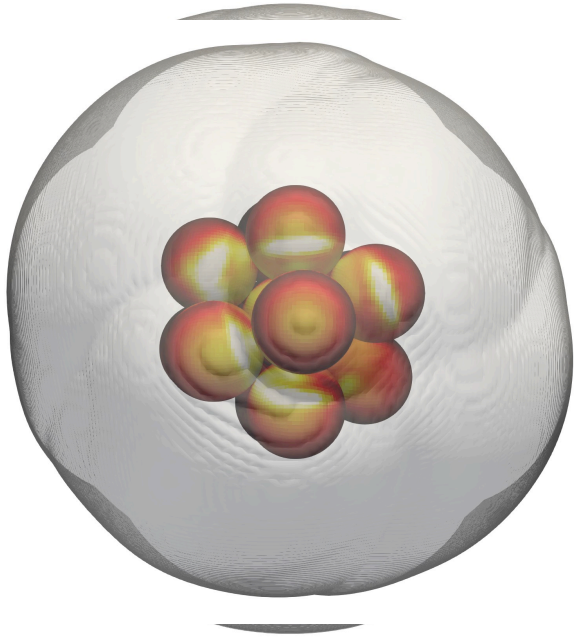


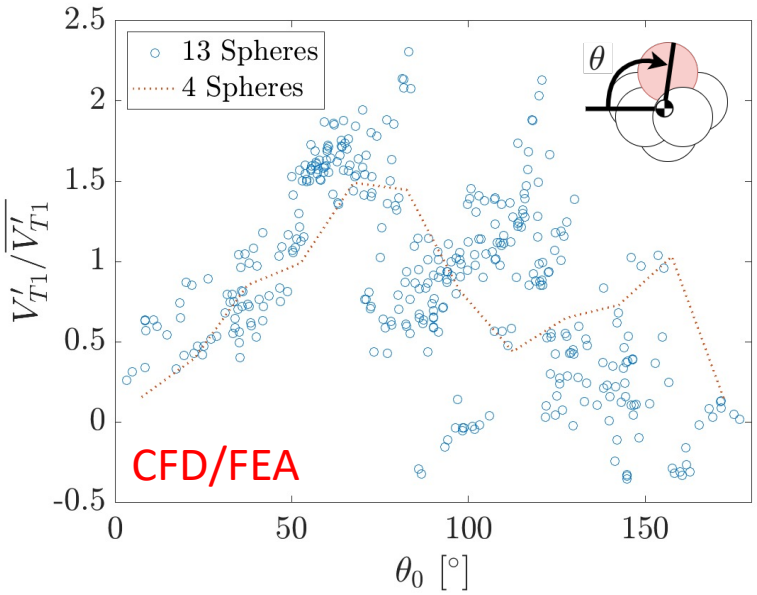
DOWNSTREAM



Primary Separation

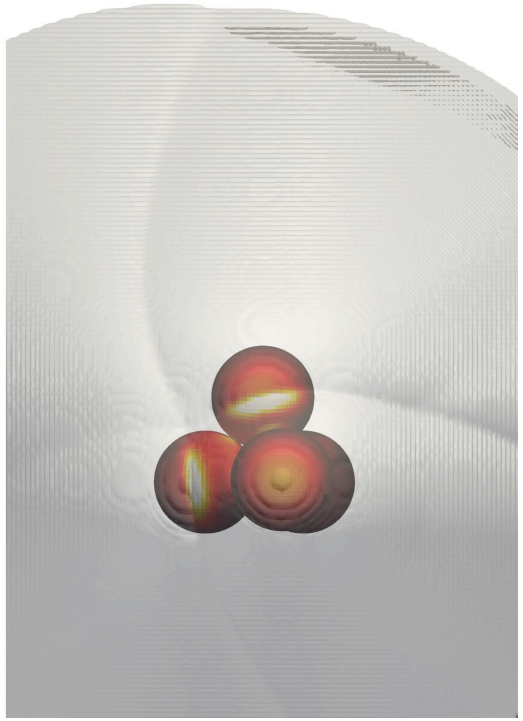
- Driven by random shock impingement patterns
  - Persists to high cluster populations
- Despite apparent randomness, lateral velocity correlated to initial polar position
  - Angular dependence shifts between 4 and 13 bodies
- Separation timescale diminishes with population
  - Decoupling radius approx. constant at $2r_0$

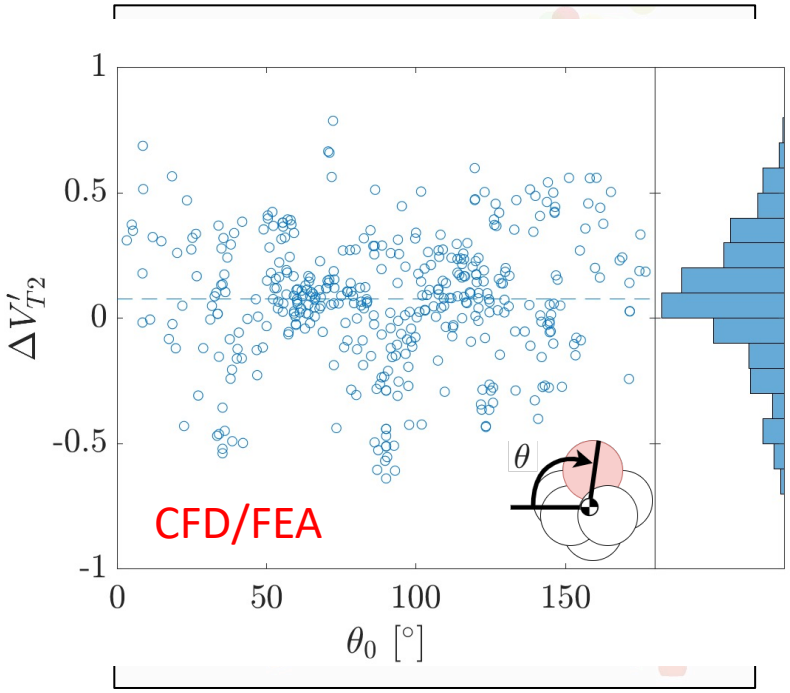


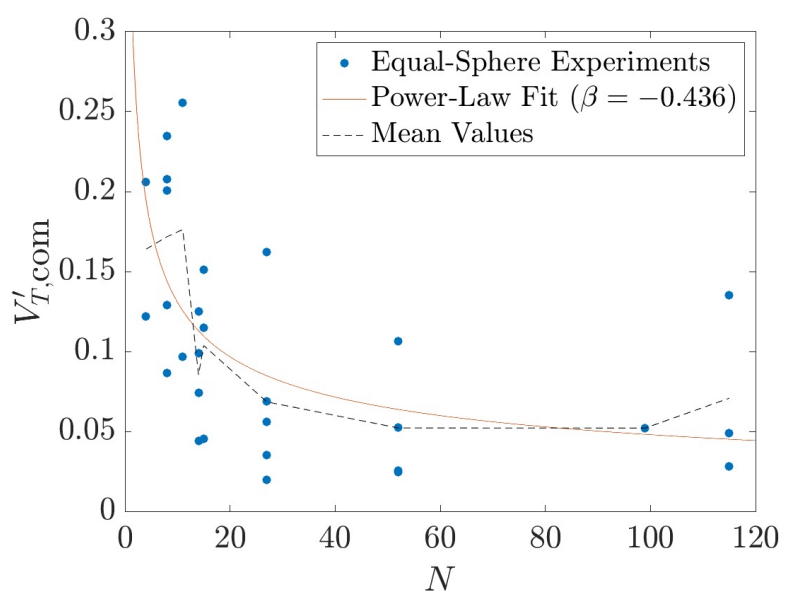


Secondary Separation

- Subcluster interactions for equal spheres dominated by wake entrainment and collisions
- Helps disperse clustered core of populous swarms
- Less prominent dynamically for high N
  - Center-of-mass offset velocity diminishes as power law
- Induces normally distributed velocity change



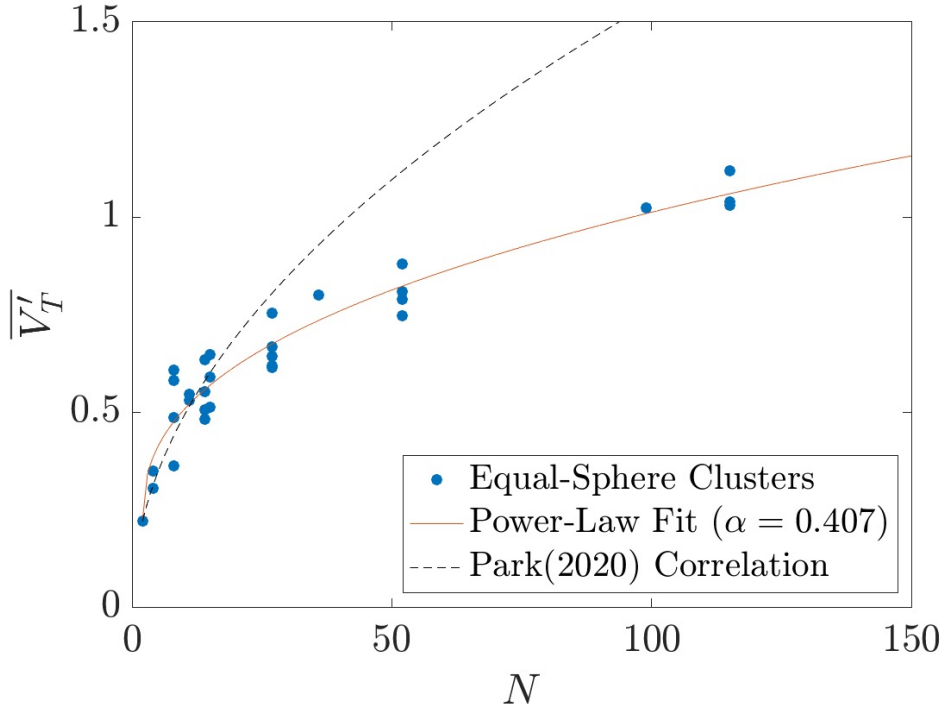




Population–Velocity Correlation

- Compute final separation velocity for each test
- Fit power-law to separation velocity
  - Force fit to pass through prescribed N=2 value
  - Obtain index of 0.407, compare with 0.5 of Park (2020) for 3,4,6-sphere tests
  - Coefficient of 0.123
- Lateral velocity for currently accepted models:
  - Discrete fragments: 0.2
  - Debris cloud: 1.8
- Diverges, not applicable to debris cloud

$$\overline{V_T'} = C(N-2)^{\alpha} + \overline{V_{T,N=2}'}$$

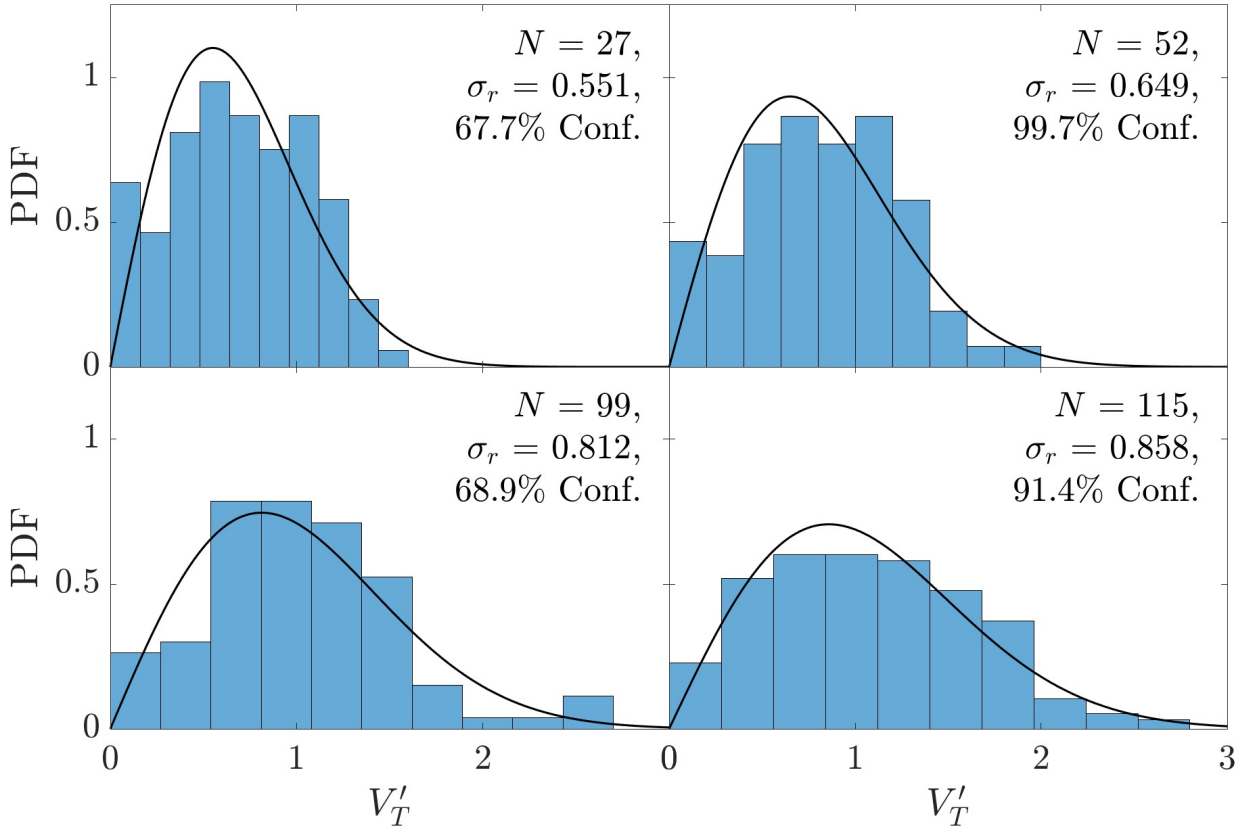


Velocity Distributions

- Preferred V_T' distribution?
- Stack lateral velocities of all tests for various populations (27, 52, 99, 115 sph)
- Resembles Rayleigh distribution:

$$f_r(V_T'; \sigma_r) = \frac{V_T'}{\sigma_r^2} e^{-V_T'^2/(2\sigma_r^2)}$$

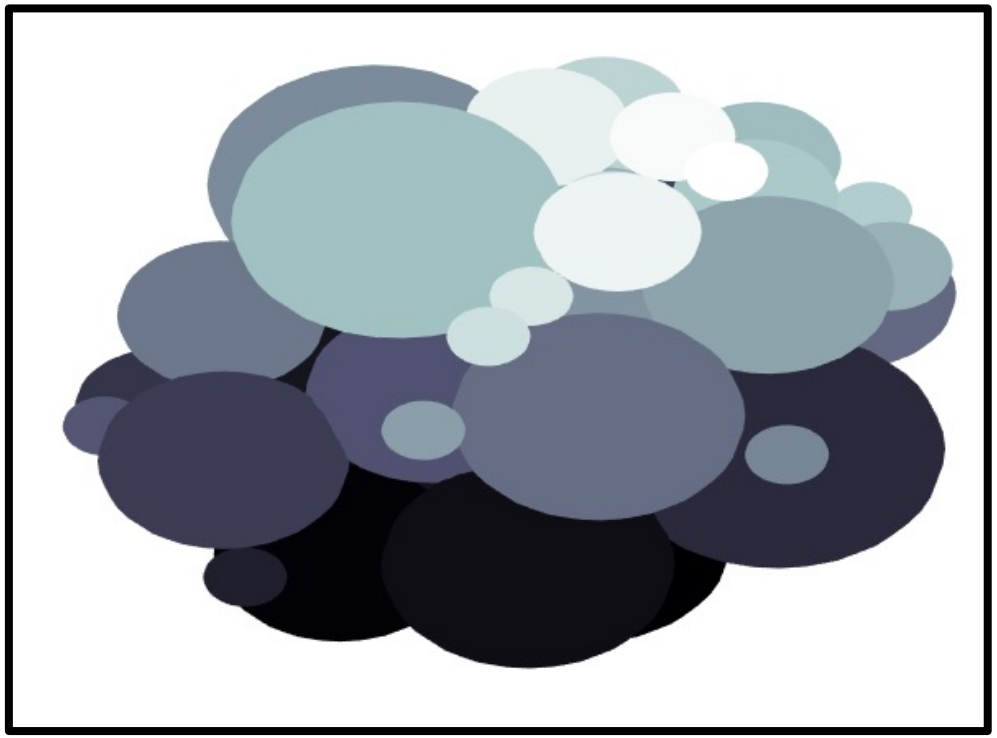
- Fits all recovered data well
- No theoretical motivation for this description of sphere separation, but useful for modeling
- For Rayleigh, mean V_T' scales linearly with σ



$$\overline{V_T'} = \sigma_r \sqrt{\frac{\pi}{2}}$$

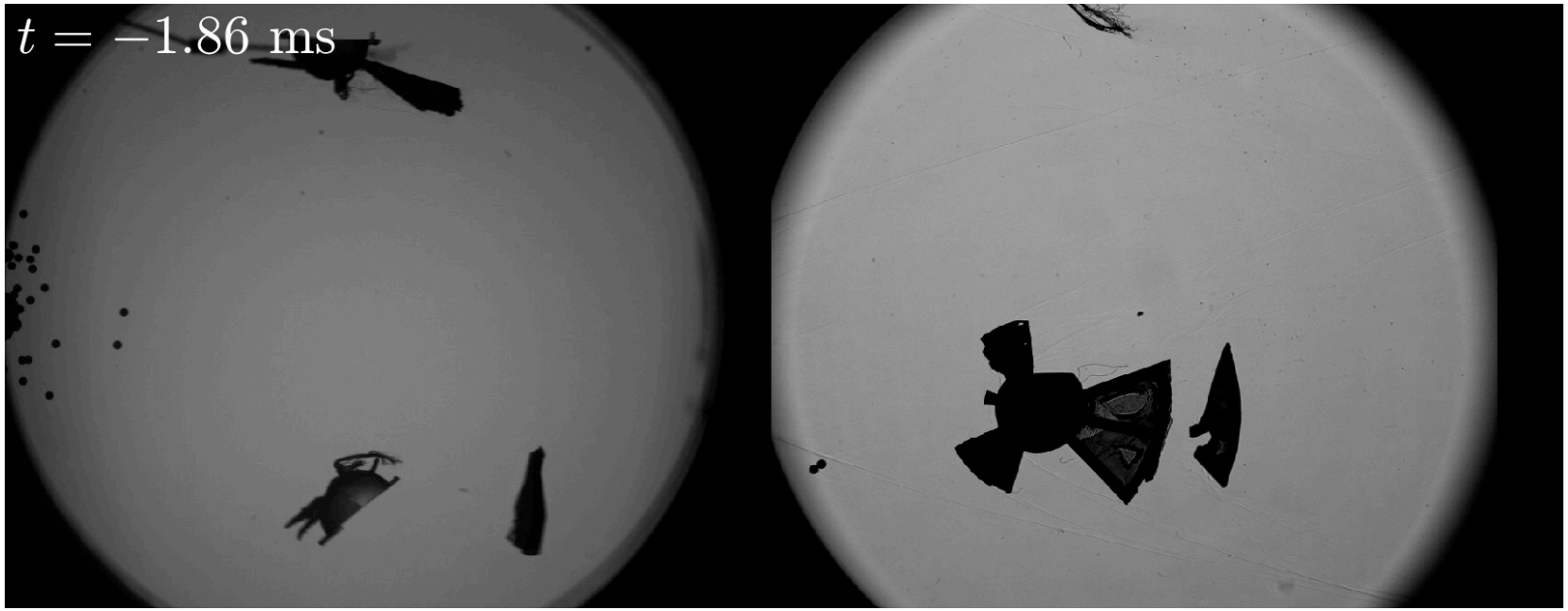
Outline

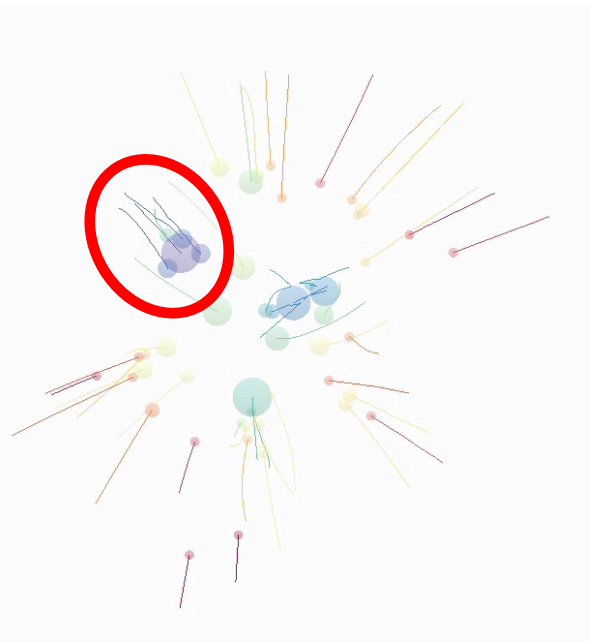
- Motivation/Approach
- Methodology
- Equal-Sphere Clusters
- Unequal-Sphere Clusters
- Dusty Debris
- Conclusions



Unequal-Sphere Clusters

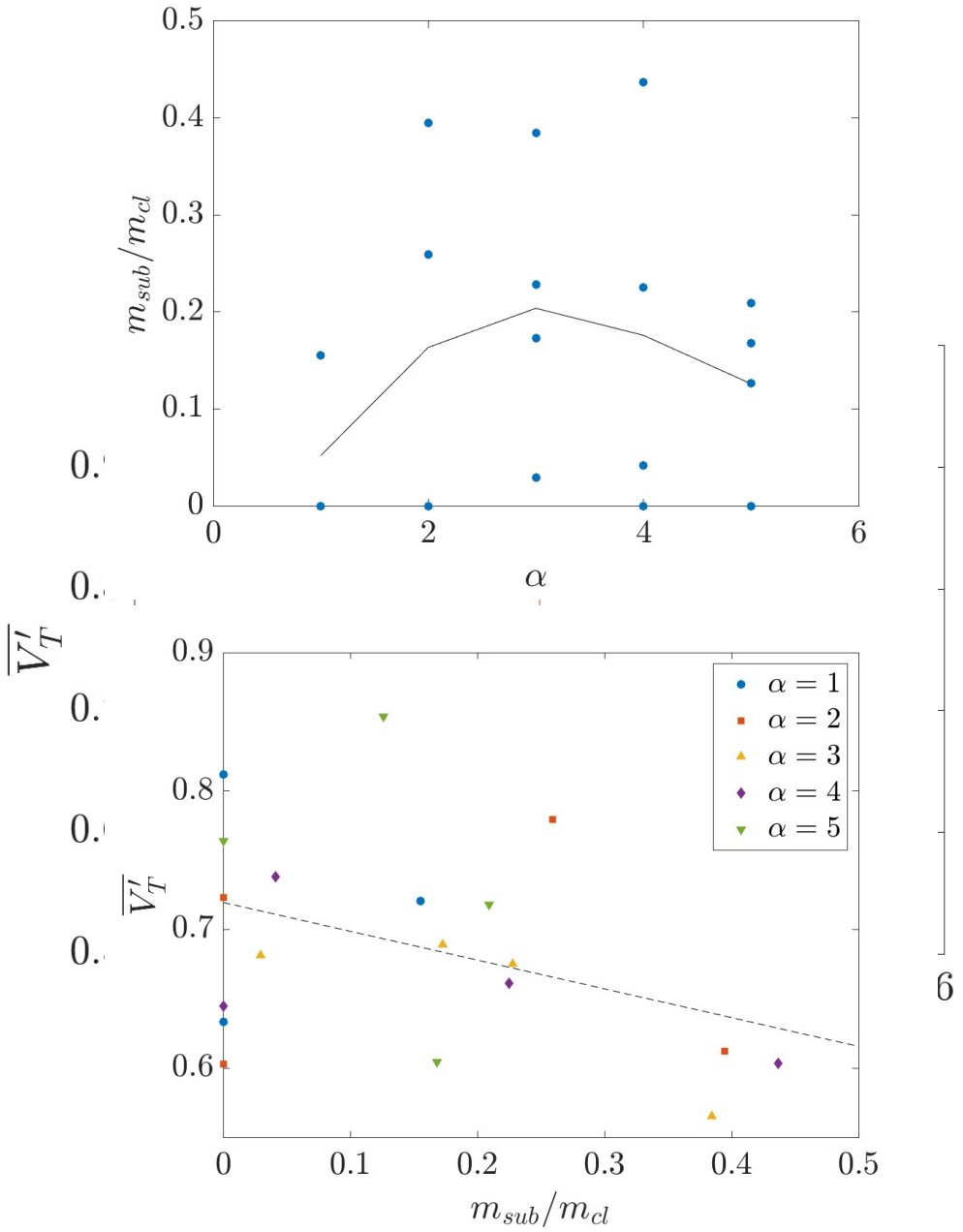
- Sample case: $\alpha = 2$
- High ejection velocities, but more entrained mass
- Stable drafting configuration?





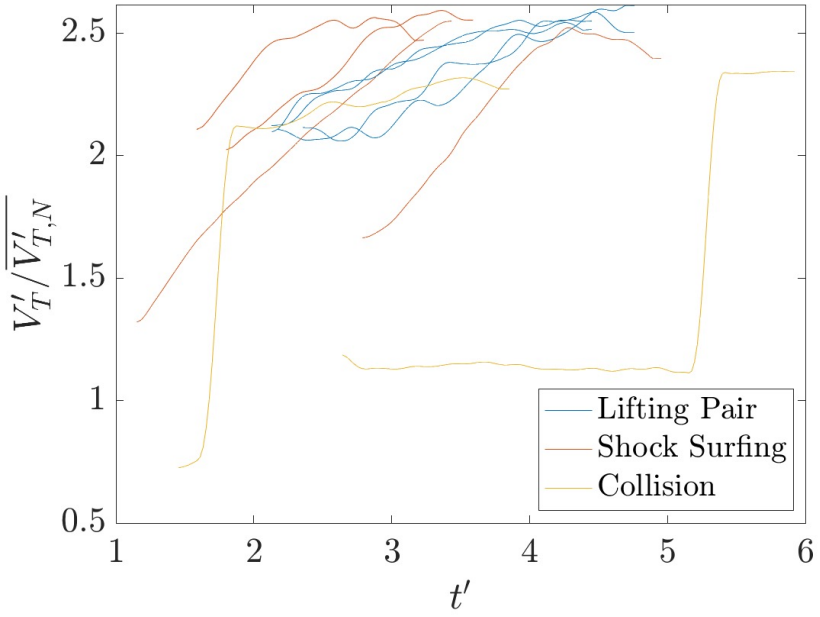
Unequal Cluster Velocities

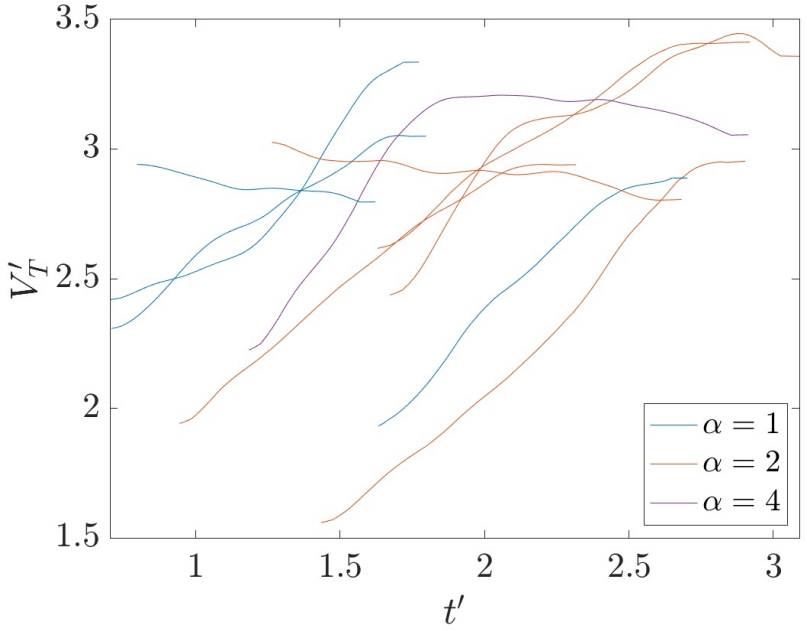
- Compare mass-weighted collective lateral velocity with 52 equal spheres
- Systematic reduction in separation rate
- Effect of mass entrainment more significant than added expulsion of smallest bodies
- For likely range of α = 3 – 4, equivalent to ~20% reduction in momentum shift from principal axis



Highly Expelled Fragments

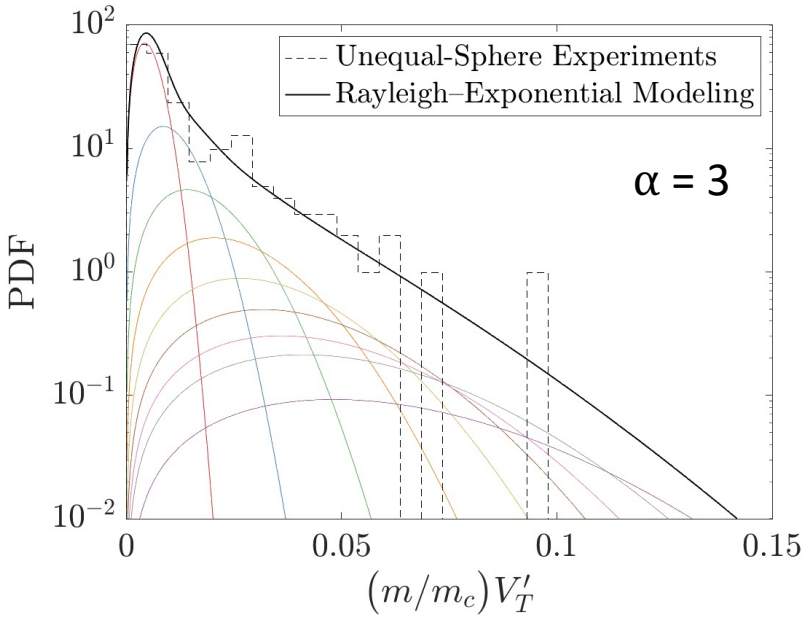
- What are the highest ejection speeds and mechanisms?
- Equal spheres: mixture of lifting pairs, shock surfing, and collisions
- Unequal spheres: all shock surfing, attain higher overall separation

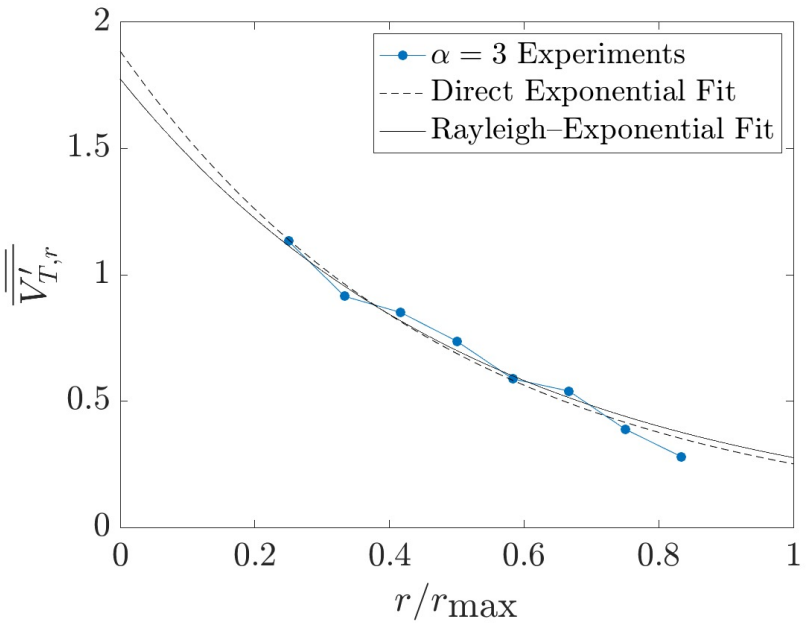




Unequal Cluster Velocities

- More important: where do spheres of a particular size end up?
- Statistical modeling process (for each α):
  - Assume each radius bin is fit by Rayleigh
  - Assume Rayleigh parameter is fit by exponential
  - Fit exponential to minimize difference between modeled and observed mass-weighted lateral vel.
- Some deviation in optimized exponential fit, as lateral velocities not perfect Rayleigh dists.
- Means/deviations from model match experiments well
  - PDFs show some disagreement though





General Lateral Velocity Prediction

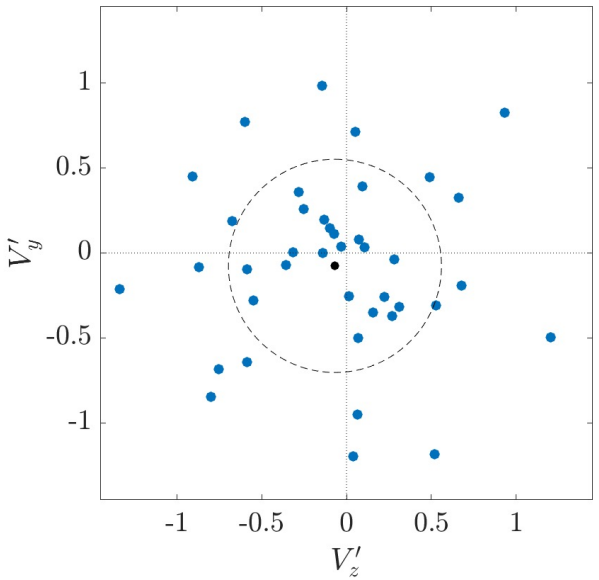
- Method for modeling velocity of arbitrary cluster composition (within problem constraints)
- Population and fragment-size distribution are taken as independent:
  1. For given α and N, get random realization of fragment sizes
  2. For each size, determine mean velocity from exponential fits
  3. Generate realizations of lateral velocity from Rayleigh distribution
  4. Scale lateral velocities by cluster population
  5. Select velocity azimuth from uniform distribution

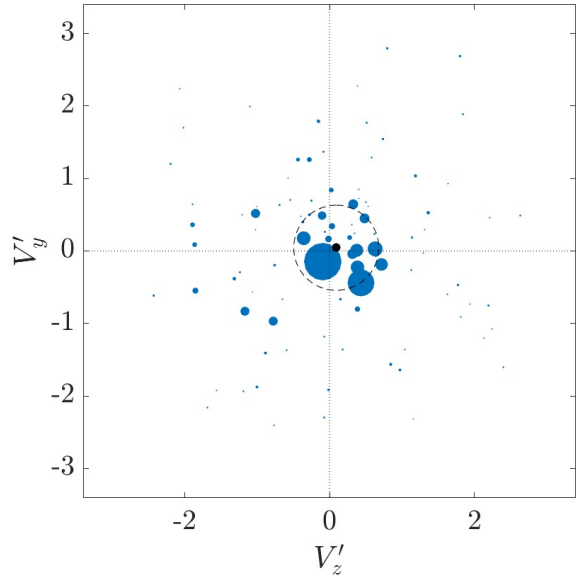
$$\overline{V'_{T,r}} = ae^{-br_s}$$

$$p(V'_T|\overline{V'_{T,r}}) = \frac{\pi}{2}\frac{V'_T}{\overline{V'_{T,r}}^2}e^{-\pi V'^2_T/(4\overline{V'_{T,r}}^2)}$$

$$V'_T \rightarrow V'_T\frac{\overline{V'_{T,N}}}{\overline{V'_{T,N=52}}} \quad \text{where} \quad \overline{V'_{T,N}} = C(N-2)^\alpha + \overline{V'_{T,N=2}}$$

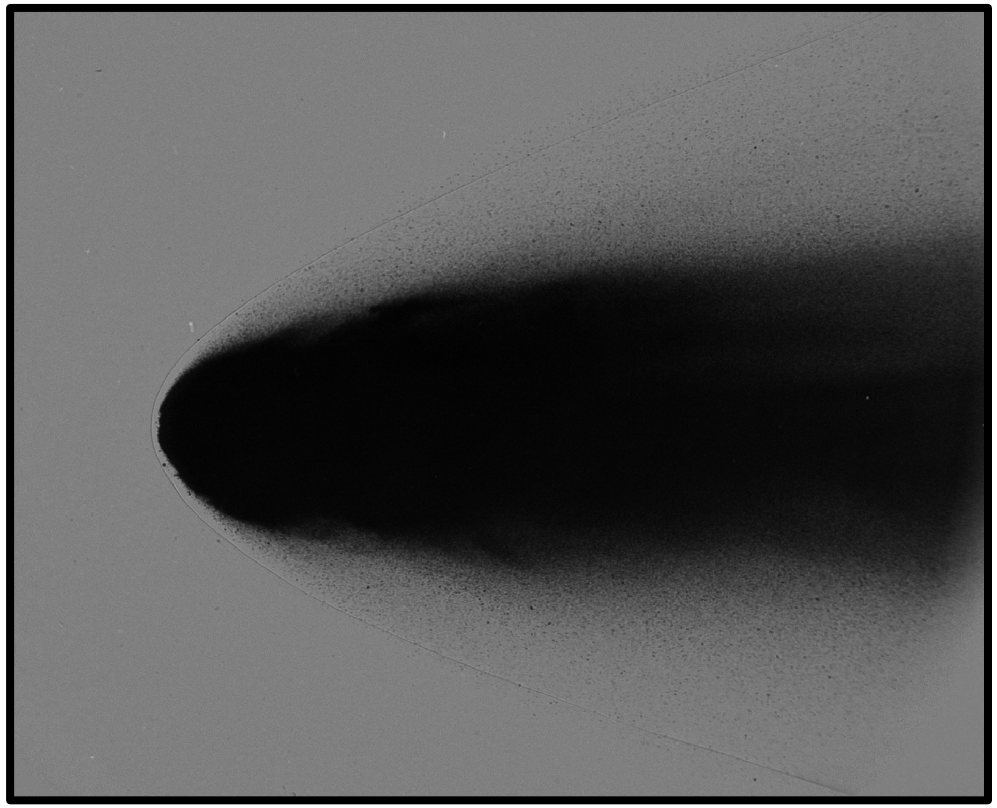
Below-left: 40 equal spheres; below-right: 100 spheres from α=3



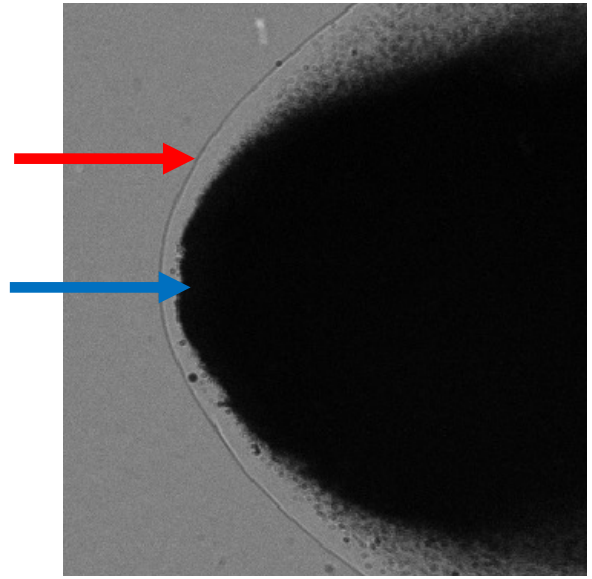


Outline

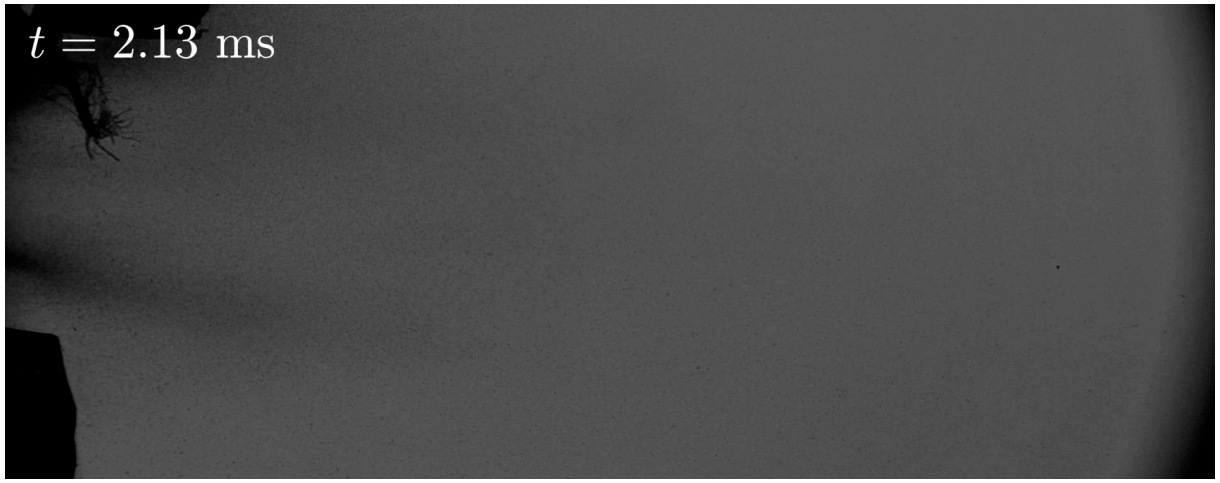
- Motivation/Approach
- Methodology
- Equal-Sphere Clusters
- Unequal-Sphere Clusters
- Dusty Debris
- Conclusions

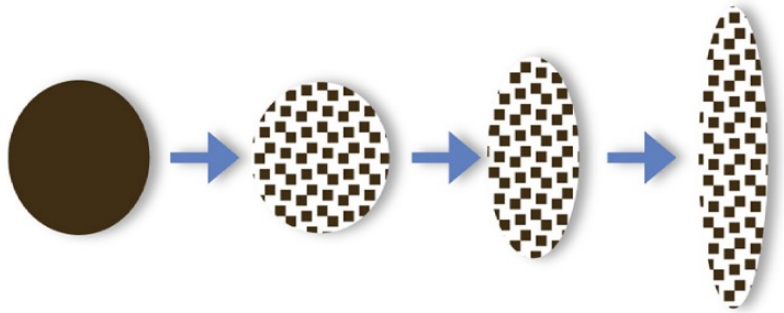


Dusty Debris



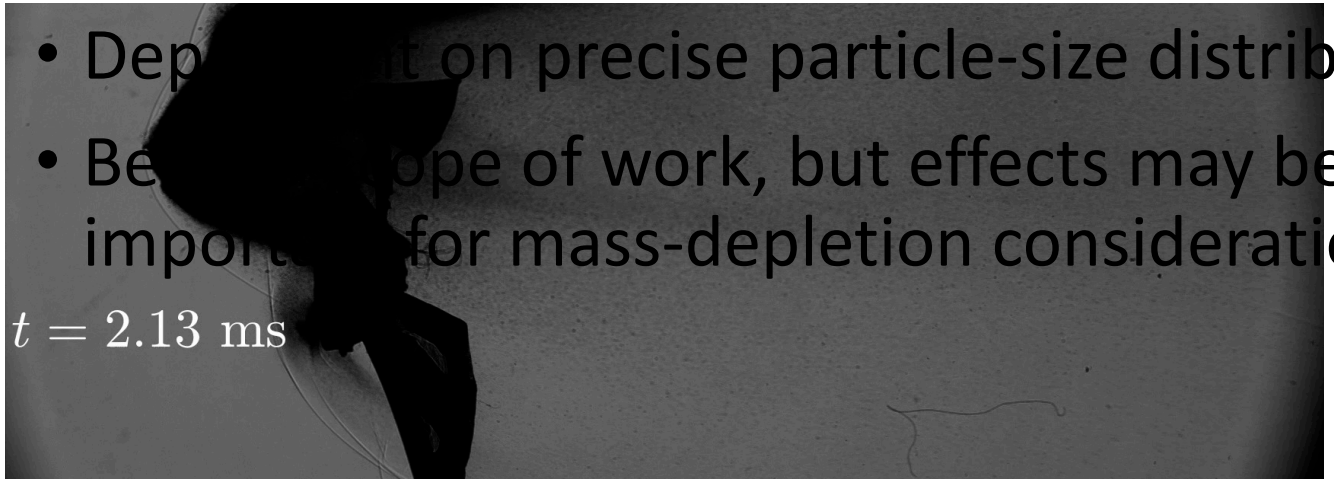
- Lateral separation much less pronounced for debris cloud
- Extended wake without highly expelled particulate
- Continuous mass loss for much of flight
- Vastly different from pancake model –> implications for energy deposition
  - Higher outboard stagnation pressure resists flattening?

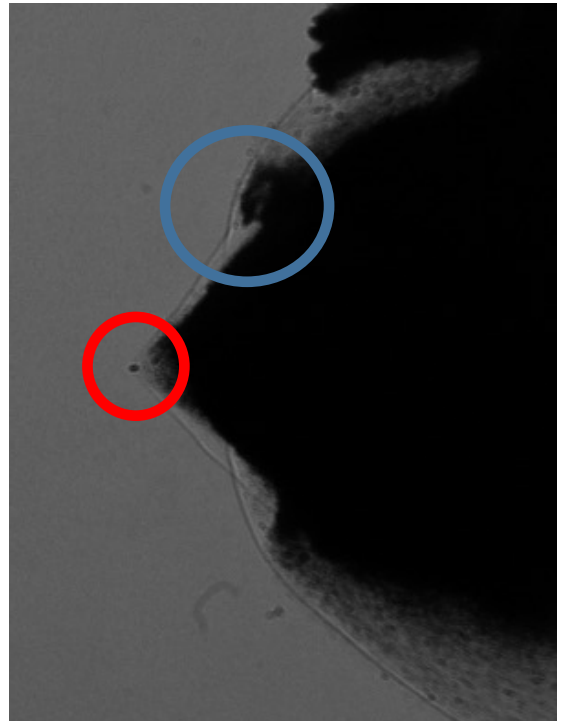


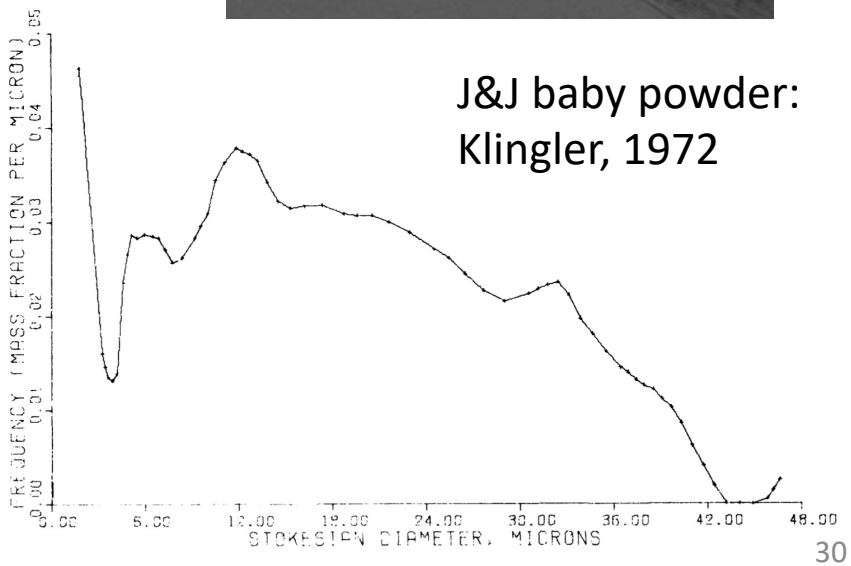


Cloud Instabilities

- In some cases, find accelerated mass depletion
- Discrete mass-loss events
- Large particle ejected ahead of cloud generates conical shock, outboard regions shed
  - Likely due to inertia and low dynamic pressure within
- Dep[illegible]t on precise particle-size distribution
- Be[illegible]ope of work, but effects may be impor[illegible]for mass-depletion considerations







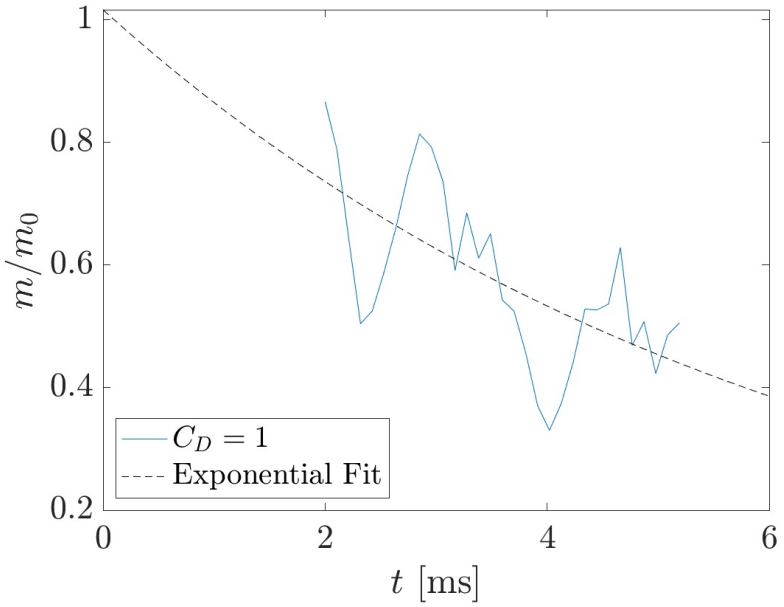
J&J baby powder:
Klingler, 1972

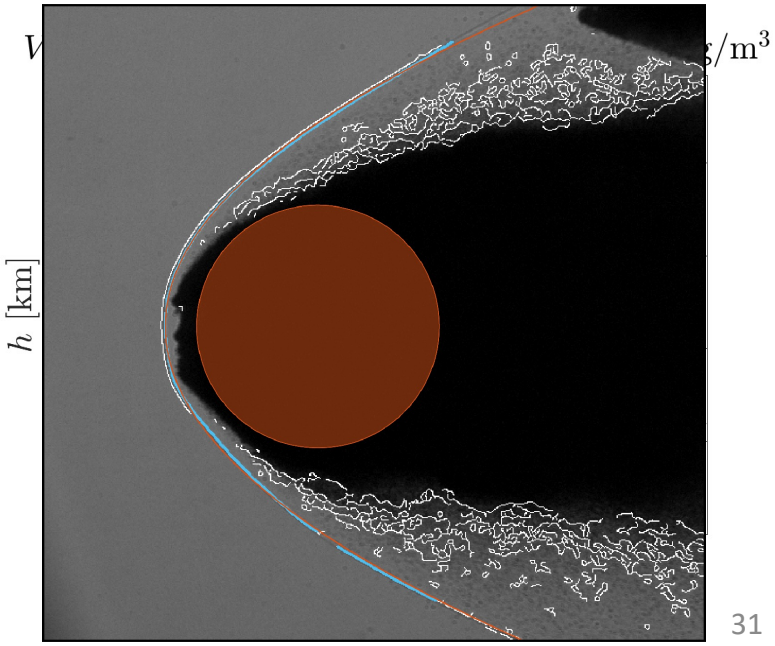
Mass Loss / Energy Deposition

- Estimate mass depletion rate
- Cross-correlate and fit shock shape in images
- Assume exponential decay in mass history for approx. constant cluster size and inflow
- Ratio of time constant to characteristic time (C = 4.43 here) gives coefficient in decay term:

$$\dot{m} = -\frac{1}{C\tau_s(u_\infty, \rho_\infty, r_c)}m$$

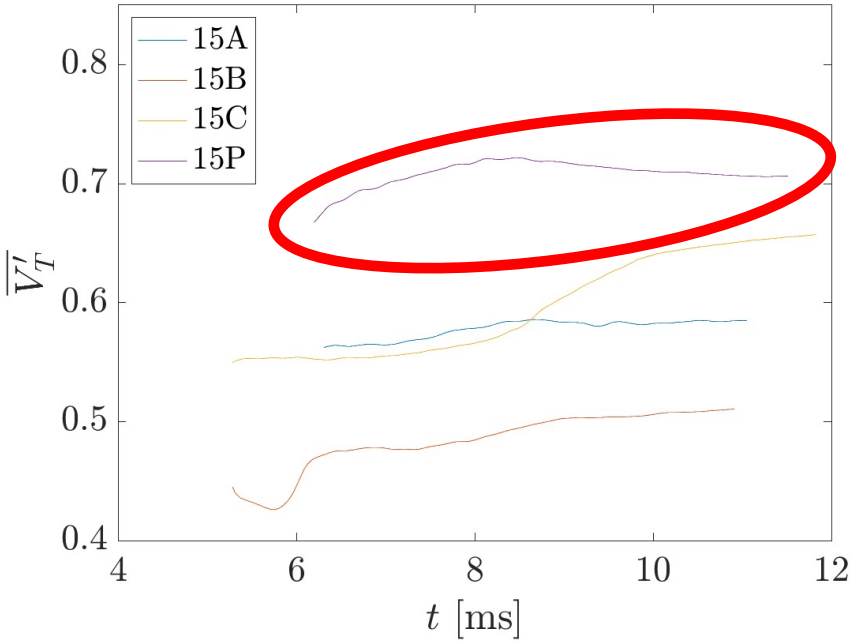
- Result: impactor penetrates further into atmosphere with less peaked deposition profile

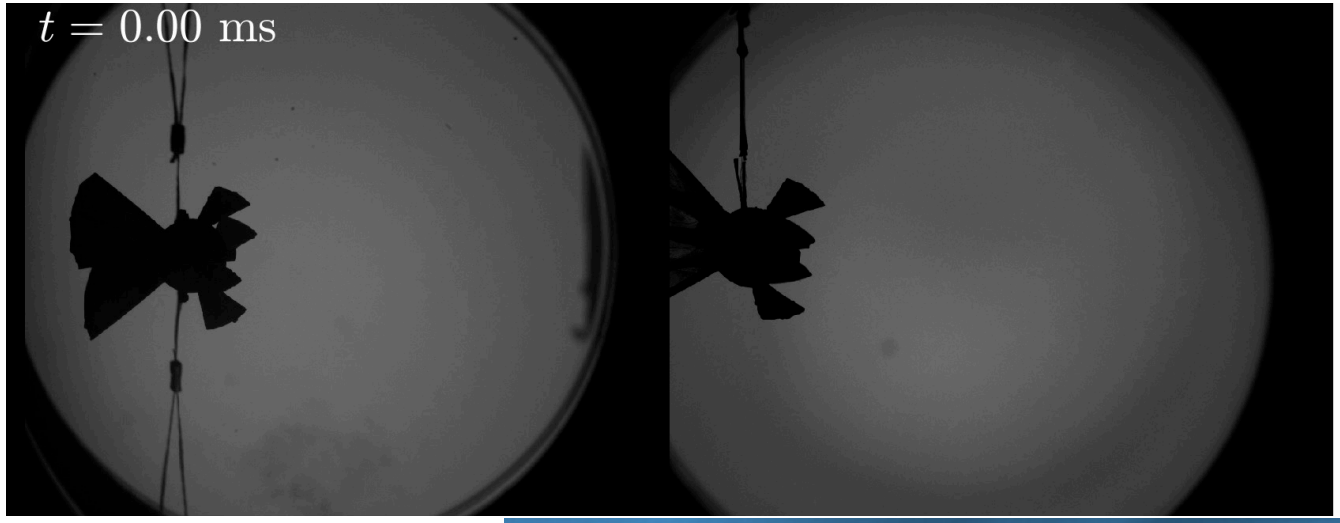


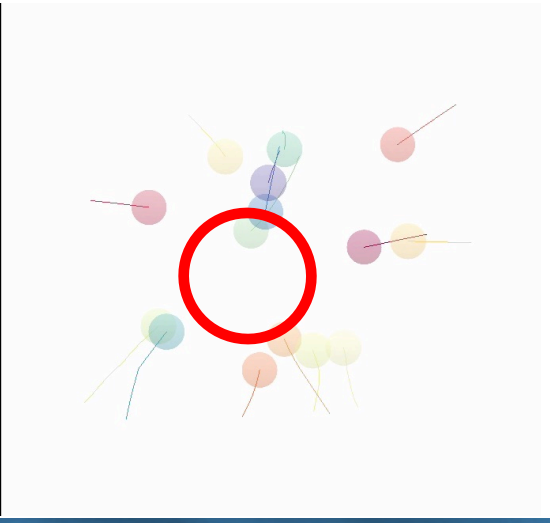


Hybrid Separation

- Most realistic treatment of meteor fragmentation
- Fill out 15-sph cluster with powder (~1/3 of total mass)
  - Lack of core on primary axis
  - V_T' is ~1.7σ above sphere-only clusters
  - Dust separates on shorter timescales as well
- Previous measurements underestimates compared to case with dust released?

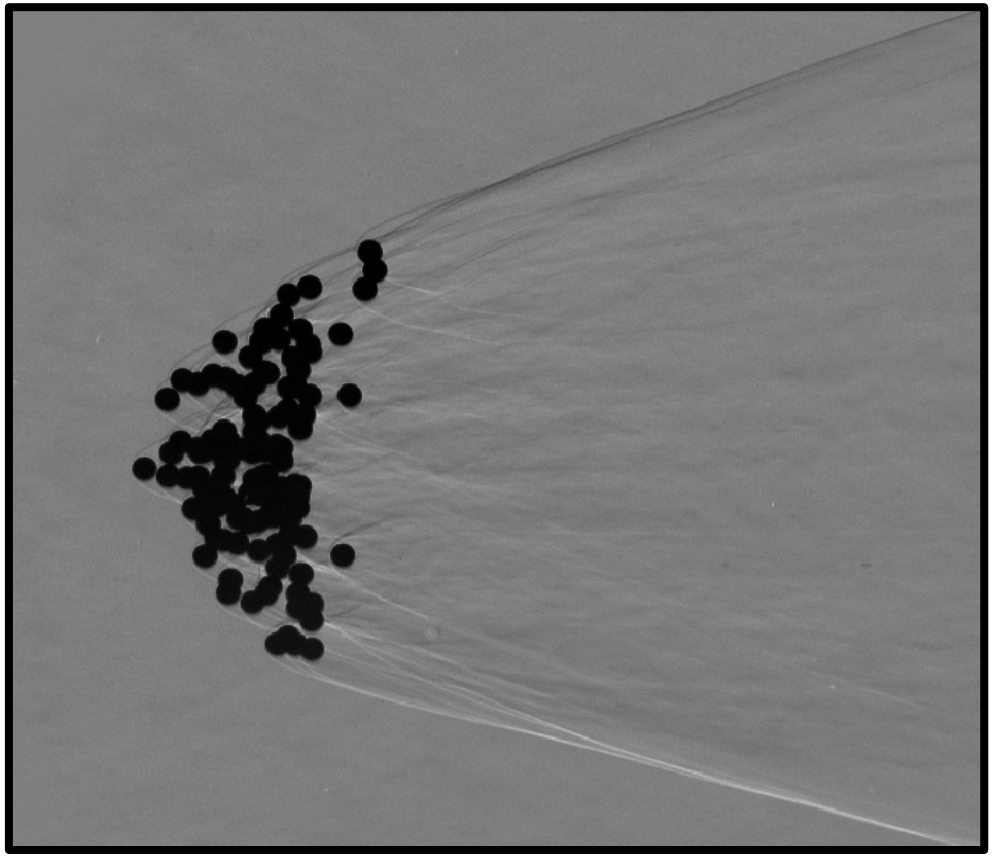






Outline

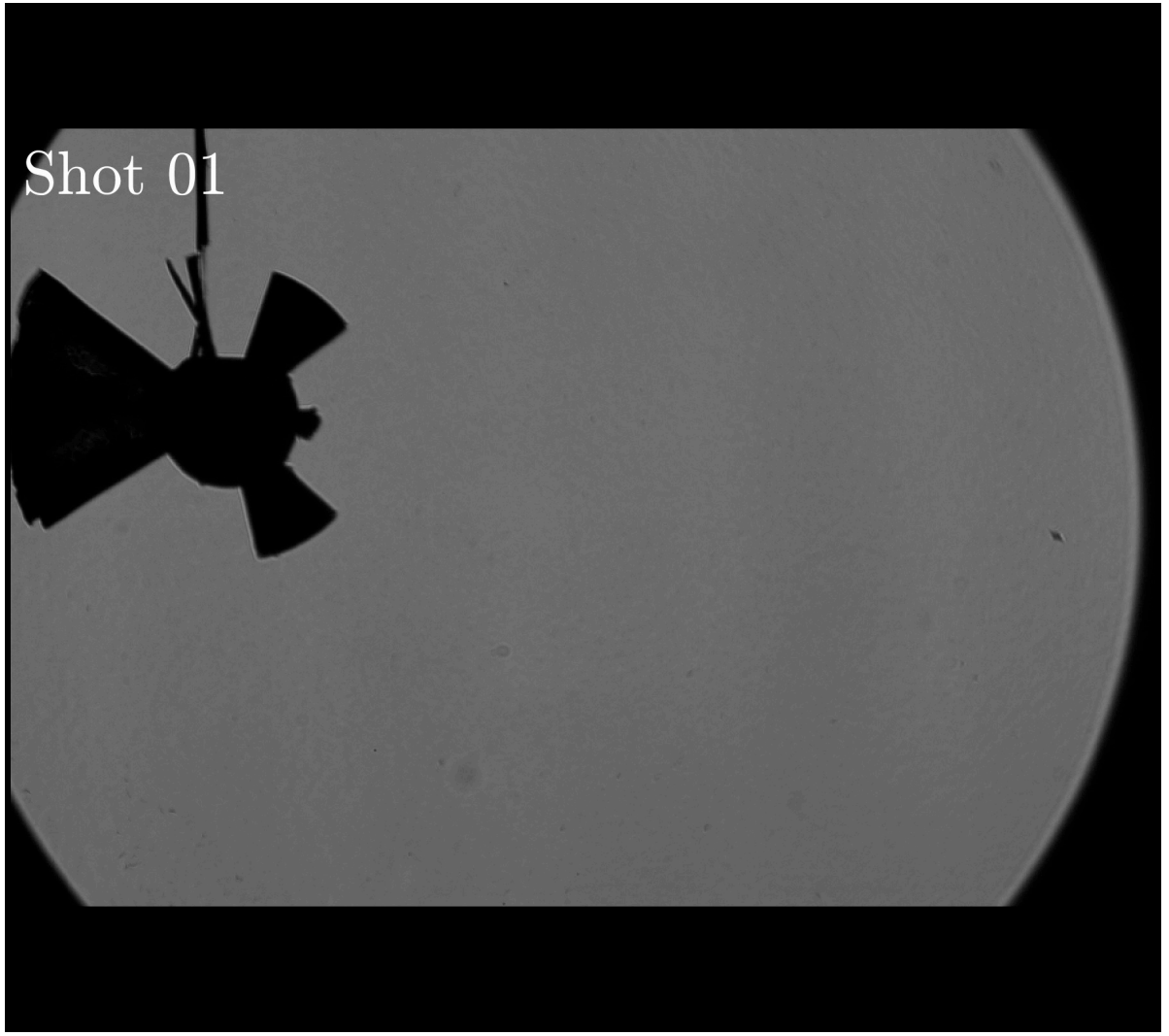
- Motivation/Approach
- Methodology
- Equal-Sphere Clusters
- Unequal-Sphere Clusters
- Dusty Debris
- Conclusions



Conclusions

- Hypersonic experimental platform enabling study of sphere cluster separation
- Lifting configuration for sphere pairs
- Identification of distinct aerodynamic regimes governing fragment trajectories
- Terminal lateral velocity statistics for range of cluster scenarios
- Distribution fits describing both equal- and unequal-sphere cluster dispersion
- Proposed empirical model for hypersonic debris dynamics

Questions?



Related Publications

- https://scholar.google.com/citations?user=Y-LtAxcAAAAJ&hl=en
- Published:
  - **Whalen, T. J.** and S. J. Laurence. Experiments on the Separation of Sphere Clusters in Hypersonic Flow. *Experiments in Fluids*, 62(4):1–19, 2021. doi:10.1007/ s00348-021-03157-z.
  - **Whalen, T. J.**, S. J. Laurence, and R. Deiterding. A Numerical Investigation of Clustered Spheres Separating in Mach 20 Flow. In *AIAA Aviation Forum*, 2020. AIAA Paper 2020-2970. doi:10.2514/6.2020-2970.
- In preparation:
  - **Whalen, T. J.**, Laurence S. J., and Deiterding, R., "Aerodynamic Separation of Sphere Clusters. Part 1. Numerical Simulations", Journal of Fluid Mechanics [Sep 2021]
  - **Whalen, T. J.**, and Laurence, S. J., "Aerodynamic Separation of Sphere Clusters. Part 2. Experiments", Journal of Fluid Mechanics [Sep 2021]
  - Register, P., Stern, E., Mathias, D., **Whalen, T. J.**, and Laurence, S. J., "Multibody Interactions between Spheres in Hypersonic Flow", Icarus Letters [Sep 2021]
  - **Whalen, T. J.** and Laurence, S. J., "Atmospheric Disruption of Dusty Debris", Journal TBD [Dec 2021]